Motorway Tidal Flow Lane Control*

Konstantinos Ampountolas, *Member, IEEE,* Joana Alves dos Santos, and Rodrigo Castelan Carlson, *Member, IEEE*

***Abstract*—The expansion of road infrastructure, in spite of increasing congestion levels, faces severe restrictions from all sorts: economical, environmental, social, or technical. An efficient and, usually, less expensive alternative to improve mobility and the use of available infrastructure is the adoption of traffic management. A particular case of interest occurs when inbound and outbound traffic on a given facility is unbalanced throughout the day. This scenario may benefit of a lane management strategy called tidal flow (or reversible) lane control, in which case the direction of one or more contraflow buffer lanes is reversed according to the needs of each direction. This paper proposes a simple and practical real-time strategy for efficient motorway tidal flow lane control. A state-feedback switching policy based on the triangular fundamental diagram, that requires only aggregated measurements of density, is adopted. A theoretical analysis based on the kinematic wave theory shows that the strategy provides a Pareto-optimal solution. Microsimulations using empirical data from the A38(M) Aston Expressway in Birmingham, UK, are used to demonstrate the operation of the proposed strategy. The robustness of the switching policy to parameter variations is demonstrated by parametric sensitivity analysis. Simulation results confirm an increase of motorway throughput and a smooth operation for the simulated scenarios.**

***Index Terms*—Tidal flow lane control, reversible lanes, bi-directional traffic, motorway traffic management, fundamental diagram of traffic.**

I. Introduction

MOTORWAY network traffic management offers a number of control measures to alleviate traffic congestion, including ramp metering, variable speed limits, driver information and route guidance, mainstream control, and lane control (see, e.g., [1], [2]). *Tidal flow (or reversible) lane control* is a type of lane management [3] that assigns a given number of lanes to one or another direction of traffic according to prevailing conditions. Modern motorway networks include various infrastructure types and emerging vehicle-infrastructure integration systems that could support tidal flow operations to improve the infrastructure efficiency in terms of throughput.

In principle, bi-directional motorways should be designed to adequately serve the peak-hour traffic volume in both directions. However, if directional flow disparity is significant between the two directions of traffic, congestion may be created in one direction while the other direction free-flows, strongly under-utilising the existing infrastructure due to the lack of efficient and comprehensive lane control. In such cases, the optimal utilisation of the existing infrastructure capacity through reversible lanes is an efficient approach to improve tidal flow traffic conditions, particularly during peak hours.

The benefit of tidal flow operation is that the available flow capacity in each direction of traffic can be varied in response to highly directional (inbound or outbound) traffic flows. An odd number of lanes, usually three to seven, is required for effective tidal flow operation. The middle lane operates as a contraflow buffer zone to serve traffic in different directions. To ensure safe operation of contraflow, lane-use control signals with green arrows and red $\times$s located at overhead gantries are used wherever a particular movement is prohibited for designated lanes. In some sites, a *barrier transfer machine* or *zipper truck* is used to redesignate traffic lanes during rush hours to ensure safety. A serious drawback, however, is the cost to manage and to efficiently control reversible lanes as well as the confusion to drivers and safety.

Nowadays, a number of sites employ tidal flow operations, including the A38(M) Aston Expressway in Birmingham, A15 Canwick Road in Lincoln, and A61 Queens Road/A61 London Road in Sheffield (UK); Sierichstraße in Hamburg (Germany); A1/A6 motorways between Diemen and Almere Havendreef, and the Coen-tunnel on the A10 (The Netherlands); SE-30 freeway in Seville (Spain); Kneza Miloša Street in Belgrade (Serbia); two arterials in Shenzhen, some freeways in Beijing, Nanjing, Changsha, and Lyuyou road in Jinan (China); many wide boulevards and some freeways in Washington, D.C., Coronado Bridge in San Diego, Tidal Busway in Eugene Oregon, and Kennedy Expressway in Illinois (USA); some boulevards in Montreal and Quebec (Canada); Auckland Harbour Bridge in Auckland (New Zealand); Sydney (Australia); a dozen of urban roads in Rio de Janeiro and São Paulo, and a section of State Road SC-405 in Florianópolis (Brazil).

Worldwide the most common practice for tidal lane operation is manual (evidence-based through empirical observations from CCTV surveillance cameras) or fixed-time control (e.g., to accommodate tidal flows associated with the AM and PM peaks) [4], [5], [6]. While in the first case it is particularly difficult for a human operator to evaluate the costs incurred by the transition period [7], in the second case, typically, a static problem of lane reversal is solved [8], [9]. These types of operation very often result in too early or too late reversal which have a negative effect on system performance [6], [10]. A number of real-time tidal flow strategies have been proposed for urban arterials [11], for motorways or uninterrupted facilities [10], [12], [13], [14], or both [7]. Except for [14] who proposed a simple logic-based strategy, all proposed strategies are rather sophisticated or require advanced technologies.

This work extends a simple and practicable strategy for smooth and efficient tidal flow operations [15]. The proposed

*This work was supported from a *Research Mobility* grant funded by CONFAP/FAPESC (Brazil) and Newton Fund (UK), and by CNPq (Brazil).

K. Ampountolas is with the James Watt School of Engineering, University of Glasgow, Glasgow G12 8QQ, United Kingdom (e-mail: konstantinos.ampountolas@glasgow.ac.uk).

J. A. dos Santos and R. C. Carlson are with the Department of Automation and Systems, Federal University of Santa Catarina, Florianópolis – Santa Catarina 88040-900, Brazil (e-mail: joana97santos@gmail.com; rodrigo.carlson@ufsc.br).

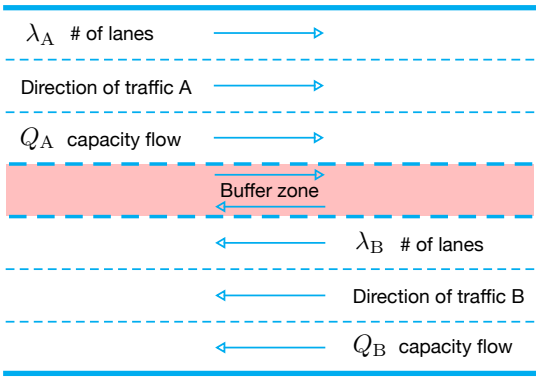

Fig. 1. A bi-directional motorway stretch with a contraflow buffer zone.

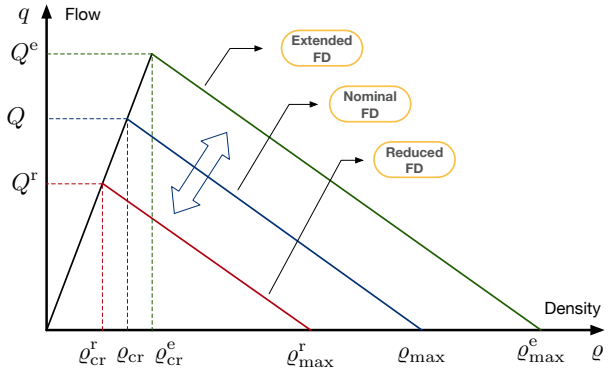

Fig. 2. Tidal flow described by three triangular fundamental diagrams.

state-feedback switching policy is based on certain properties of the triangular (piece-wise linear) fundamental diagram (FD) of motorway traffic and relies on real-time measurements of density only (or proxies of density, such as occupancy and speed). It is, thus, applicable in real-time to improve the bi-directional infrastructure efficiency. This paper also presents a theoretical analysis of tidal traffic flow that is based on the Kinematic Wave Theory (KWT). This analysis provides a number of insights on the effectiveness of tidal flow lane management in terms of flow capacity, throughput maximisation, and total time spent.

The rest of the paper is organised as follows. Section II introduces the motorway tidal flow lane control problem and presents the proposed FD-based policy. A theoretical analysis of the proposed strategy is presented in Section III. Section IV presents a microsimulation study of the application of the proposed approach to the A38(M) Aston Expressway (Birmingham, UK). The case study benefits from real empirical data collected from a number of loop detectors in the studied site. Conclusions are given in Section V.

II. Motorway Tidal Flow Lane Control

Consider a bi-directional motorway stretch with a contraflow buffer zone as shown in Fig. 1. The buffer lane is highlighted with red surfacing and permits tidal flow operations. The tidal (or reversible) lane switches direction at peak periods to provide extra capacity in one direction (either A or B). Typically, this changes to four lanes in one direction and two lanes in the opposite direction maintaining the one lane buffer for safety reasons. In case of limited infrastructure (e.g., three lanes with one buffer lane) or motorway stretches with lane speed control, the buffer lane can be assigned to the appropriate direction of traffic without any other lane closure.

For analysis, it is convenient to assume that, under stationary traffic conditions, the bi-directional motorway stretch indicates a triangular nominal FD (nFD) as shown in Fig. 2. This theoretical model has the feature of being piecewise linear but not smooth, i.e., not having continuous derivatives. It has been proposed for the first time by Newell [16] as an alternative (simplified kinematic wave theory) to solve the Lighthill-Whitham-Richard (LWR) model [17], [18], while it fits well with field empirical data as demonstrated in a number of practical studies (see e.g., [19]). In the same vein, we define two other diagrams, namely reduced FD (rFD) and extended FD (eFD), to characterise tidal traffic flow operations. In particular under tidal flow lane control, the eFD characterises the traffic conditions in the direction of traffic with extra capacity, while the rFD characterises the opposite direction of traffic with reduced capacity. For simplicity, all FDs assume the same forward kinematic wave speed $w_f = v_f$, with v_f the free flow speed (the slope of the left branch of the triangular FD), although different free-flow speeds or generic unimodal FDs can be assumed as appropriate (see Section III). Schematically, the proposed control logic is illustrated with a bi-directional arrow in Fig. 2. It relies on the gentle switching of the nFD to eFD or rFD under tidal flow lane control. It should be noted that all the FDs (nFD, rFD, and eFD) can be readily estimated off-line provided empirical data. Moreover the use of a unique fundamental diagram reflecting a single lane may not be suitable for tidal flow control. This is because the number of lanes available in each direction of traffic may have an effect on lane usage and infrastructure capacity.

The following assumption guarantees smooth and efficient switching of the nFD to eFD or rFD.

Assumption 1: If traffic conditions do not change rapidly with time, the motorway stretches A and B should not simultaneously operate in the congested regime of the nominal fundamental diagram that is nFD.

For instance, under stationary traffic conditions and operations, both directions of traffic A, B in the motorway stretch shown in Fig. 1 will operate under the nFD with number of lanes $\lambda_A = \lambda_B = \lambda$ and maximum stationary flow (or capacity) $Q_A = Q_B = Q$. Now assume that the buffer lane switches direction to provide extra capacity in one direction of traffic, let us say to direction A (respectively, B). This results in the direction A (respectively, B) operating under the eFD while the direction B (respectively, A) operates under the rFD. Note that the efficient switching from the nFD to rFD requires the prevailing flow, q, of the free-flowing direction of traffic (i.e., with states in the left branch of the FD) to satisfy $q \leq Q^r$, to avoid undesirable effects such as capacity drops in the direction of traffic with impending reduced capacity, where Q^r is the capacity of the rFD (see Fig. 2).

The developed FD-based tidal lane switching policy mon-

itors in real-time the current prevailing densities $\varrho_{\rm A}$ and $\varrho_{\rm B}$ in both directions A, B, and compare them with the critical density $\varrho_{\rm cr}$ of the nFD and $\varrho^{\rm r}_{\rm cr}$ of the rFD (see Fig. 2). If critical conditions prevail at one direction of traffic during peak hours (i.e., its density is higher than the critical density of nFD) and the other direction of traffic operates under free flow traffic conditions (i.e., its density is lower than the critical density of rFD), then the buffer lane switches direction to provide extra capacity to the crowded direction of traffic; while the nominal capacity of the opposite direction is reduced to rFD. Switching is allowed if and only if both conditions are satisfied, otherwise (i.e., if both directions of traffic are congested or both uncongested) a *do nothing policy* is applied and both directions of traffic operate under the nFD with $\lambda_{\rm A} = \lambda_{\rm B} = \lambda$. The presented control logic can be summarised in the following FD-based state-feedback switching policy:

$$u(k+1) = \begin{cases} 1, & \text{if } \varrho_{\rm A}(k) > \gamma\varrho_{\rm cr} \text{ and } \varrho_{\rm B}(k) \le \gamma^{\rm r}\varrho^{\rm r}_{\rm cr}, \\ -1, & \text{if } \varrho_{\rm B}(k) > \gamma\varrho_{\rm cr} \text{ and } \varrho_{\rm A}(k) \le \gamma^{\rm r}\varrho^{\rm r}_{\rm cr}, \\ 0, & \text{otherwise,} \end{cases} \quad (1)$$

with $k = 0, 1, 2, \ldots$ the discrete time index and u indicates the number of lanes opened or closed in each direction of traffic at the next time instant $k+1$ (see below for details). This control policy is executed in real-time every control period T, while $\varrho_{\rm A}$ and $\varrho_{\rm B}$ are aggregated over the measurements interval $T_{\rm m}$. A typical period of $T_{\rm m} = 15$ mins can be used that sustains the motorway capacity. The control period T should be sufficient large to avoid oscillations (e.g., frequent switchings) and windup phenomena (e.g., in dead zones where control does not affect the state of the system). Moreover, Assumption 1 guarantees that the proposed switching lane scheme provides smooth and efficient tidal flow control operations. The basic steps of the FD-based tidal lane switching policy are given in Algorithm 1.

Several points should be noted:

- The thresholds $\Delta \triangleq \gamma\varrho_{\rm cr}$ and $\Delta^{\rm r} \triangleq \gamma^{\rm r}\varrho^{\rm r}_{\rm cr}$ in (1) and in the "if statements" of Algorithm 1 include the parameters $\gamma \in [1, 1.5)$ and $\gamma^{\rm r} \in (.5, 1]$ to compensate for possible uncertainties associated with the pre-specified critical densities. The difference of the two thresholds defines the bandwidth of switching as $\Delta_{\rm b} \triangleq \Delta - \Delta^{\rm r}$.
- Steps 2–4 and 6–8 of the algorithm ensure smooth tidal flow operations by allocating sufficient time for clearing the contraflow buffer lane as well as one lane from either A or B directions, to serve as a new buffer lane for safety.
- The FD-based policy can work with proxies of density, e.g., occupancies (available from inductive-loop detectors), without significant modifications of the main logic.
- The FD-based policy is robust because it does not rely on any forecasts. It relies only on the current and observable densities $\varrho_{\rm A}$, $\varrho_{\rm B}$ (or proxies of the system state) and on the gentle switching of the nFD to rFD or the eFD. Thus, the policy has low requirements and can be applied with very limited knowledge of the environment, if loop-detector data are available in real-time.
- The FD-based policy can be extended in a straightforward way to account for motorways with more than one reversible lanes by an appropriate change of the flow capacity in the rFD and nFD, or by having multiple FDs and corresponding *if* statements in Algorithm 1.
- In absence of directional flow disparity (i.e. in absence of Assumption 1) and evidence of spillback congestion in both directions of traffic, the policy (1) can be extended to take into account queue lengths, similar to [14]. Additional infrastructure (detectors upstream and downstream of the prevailing bottleneck location) will be required for real-time queue surveillance, however.

Algorithm 1: FD-based Switching Policy

Data: Critical densities $\varrho_{\rm cr}$ and $\varrho^{\rm r}_{\rm cr}$ of nFD and rFD; control parameters γ and $\gamma^{\rm r}$; number of lanes λ; control interval T; measurements interval $T_{\rm m}$
Result: Control $u(k+1)$; $\lambda_{\rm A}(k+1)$, $\lambda_{\rm B}(k+1)$
Initialise: Set $k \leftarrow 0$; $u(k) \leftarrow 0$; $\lambda_{\rm A}(k), \lambda_{\rm B}(k) \leftarrow \lambda$;
begin
1 Enter new measurements $\varrho_{\rm A}(k)$ and $\varrho_{\rm B}(k)$ (aggregated over $T_{\rm m}$);
if $\varrho_{\rm A}(k) > \gamma\varrho_{\rm cr}$ ***and*** $\varrho_{\rm B}(k) \le \gamma^{\rm r}\varrho^{\rm r}_{\rm cr}$ **then**
2 Close access to buffer and B's current median lane;
3 Wait until both lanes are empty;
4 Open buffer lane for A's access;
5 Set $u(k+1) \leftarrow 1$;
else if $\varrho_{\rm B}(k) > \gamma\varrho_{\rm cr}$ ***and*** $\varrho_{\rm A}(k) \le \gamma^{\rm r}\varrho^{\rm r}_{\rm cr}$ **then**
6 Close access to buffer and A's current median lane;
7 Wait until both lanes are empty;
8 Open buffer lane for B's access;
9 Set $u(k+1) \leftarrow -1$;
else
10 Set $u(k+1) \leftarrow 0$; do nothing;
end
11 Set $\lambda_{\rm A}(k+1) \leftarrow \lambda + u(k+1)$;
12 Set $\lambda_{\rm B}(k+1) \leftarrow \lambda - u(k+1)$;
13 Set $k \leftarrow k+1$; go to step **1**;
end

As a final remark, the proposed FD-based policy (1) guarantees that both directions of traffic operate in the uncongested regime of either the nFD or rFD and eFD, which is described by a forward kinematic wave speed $w_{\rm f}$ (the left branch of any triangular FD in Fig. 2), provided the total upstream demand in both directions of traffic does not exceed the motorway capacity as a whole and per direction. As a special property of the triangular FD, free flow speed $v_{\rm f}$ applies to all uncongested conditions and thus $w_{\rm f} = v_{\rm f}$.

III. Kinematic Wave Theoretical Analysis

The following analysis based on the Kinematic Wave Theory (KWT) provides a number of insights on the effectiveness of the proposed FD-based switching policy in terms of motorway capacity and throughput maximisation, and total time spent. The main question to address is: if inflows and outflows

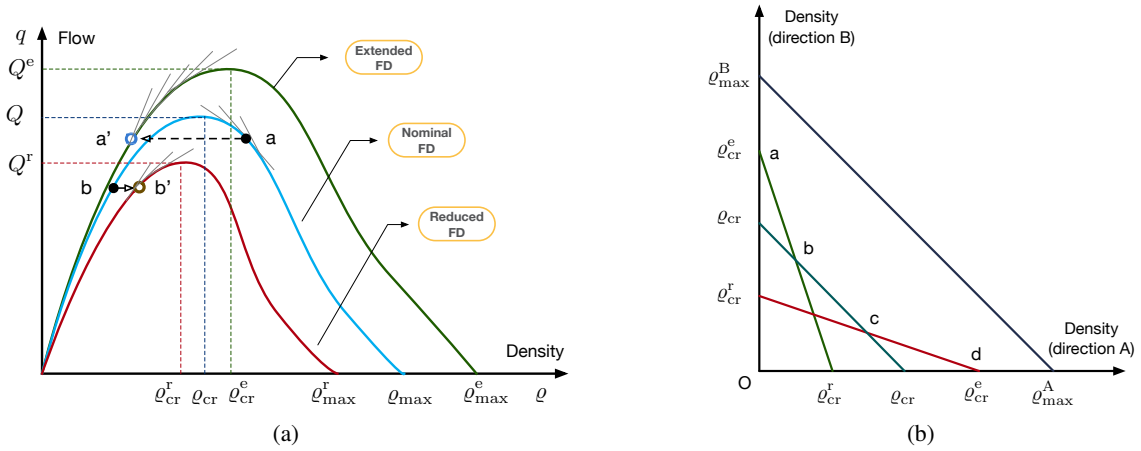

Fig. 3. (a) Tidal flow operations described by three FDs; (b) Pareto efficient solutions in $(\varrho_{\mathrm{A}}, \varrho_{\mathrm{B}})$ phase diagram. Region "abcd" is the Pareto frontier.

are balanced to maintain the bi-directional traffic in a steady-state for a fixed total number of desired bi-directional trips, what is the distribution of densities that maximises the bi-directional total outflow and how the infrastructure should be managed to accommodate this distribution?

Consider the closed (no on/off-ramps) bi-directional motorway stretch shown in Fig. 1 of length ℓ with a variable number of lanes in each direction of traffic and different input demands. Define $\ell_{\mathrm{A}} \triangleq \ell \cdot \lambda_{\mathrm{A}}$ and $\ell_{\mathrm{B}} \triangleq \ell \cdot \lambda_{\mathrm{B}}$ to be the vertical lengths of stretches A and B, respectively. Note that ℓ_{A} and ℓ_{B} are variable but bounded, given one buffer lane. Their length depends on the number of lanes assigned in each direction of traffic while ℓ is bounded by the existing infrastructure. Direction of traffic is denoted with A or B as in Fig. 1.

Let $\varrho_{\mathrm{A}}(x)$ and $\varrho_{\mathrm{B}}(y)$ be the density at location x and y, respectively. Let $F(\varrho_{\mathrm{A}}(x), x)$ and $G(\varrho_{\mathrm{B}}(y), y)$ be two location-dependent concave FDs that provide the outflow (throughput) at x and y when the local density is $\varrho_{\mathrm{A}}(x)$ and $\varrho_{\mathrm{B}}(y)$, respectively. Assume that the downstream infrastructure (off-ramps, exit-points, etc.) has enough capacity to discharge any desired outflows in both directions of traffic. Now assume that there is some directional flow disparity between the two directions of traffic and thus define as $f(x) = f(x, x+dx)/dx$ and $g(y) = g(y, y+dy)/dy$ the fraction of traffic exiting per unit length of road at x and y, respectively. Then, the prevailing bi-directional outflow in an interval $i_{x,y} = (x, y \mid x+dx; y+dy)$ is the sum of two products: (a) the product of the flow $F(\varrho_{\mathrm{A}}(x), x)$ and the fraction of vehicles $f(x)dx$ exiting in $i_{x,0}$; (b) the product of the flow $G(\varrho_{\mathrm{B}}(y), y)$ and the fraction of vehicles $g(y)dy$ exiting in $i_{0,y}$. Thus the total bi-directional outflow is given by:

$$O = \int_0^{\ell_{\mathrm{A}}} F(\varrho_{\mathrm{A}}(x), x) f(x)\, dx + \int_0^{\ell_{\mathrm{B}}} G(\varrho_{\mathrm{B}}(y), y) g(y)\, dy. \quad (2)$$

Provided the flow disparity between the two directions of traffic, the total bi-directional accumulation of vehicles is

$$N = \int_0^{\ell_{\mathrm{A}}} \varrho_{\mathrm{A}}(x)\, dx + \int_0^{\ell_{\mathrm{B}}} \varrho_{\mathrm{B}}(y)\, dy. \quad (3)$$

The problem of bi-directional throughput maximisation now reads: maximise (2) subject to (3), where $\varrho_{\mathrm{A}}(x)$ and $\varrho_{\mathrm{B}}(y)$ are the variables to be optimised. This problem can be readily solved by introducing the Lagrangian associated with the constrained problem and then taking the appropriate partial derivatives equal to zero (provided $\varrho_{\mathrm{A}}(x) > 0$, $\varrho_{\mathrm{B}}(y) > 0$). From the first-order necessary conditions, it results that the optimal solution $\varrho^*_{\mathrm{A}}(x)$, $\varrho^*_{\mathrm{B}}(y)$ must satisfy

$$f(x) w_{\mathrm{A}}(\varrho^*_{\mathrm{A}}(x), x) = g(y) w_{\mathrm{B}}(\varrho^*_{\mathrm{B}}(y), y) = \mu^*, \quad (4)$$

with μ^* = constant the associated Lagrange multiplier; and, $w_{\mathrm{A}}(\varrho_{\mathrm{A}}, x) \triangleq \partial F(\varrho_{\mathrm{A}}, x)/\partial \varrho_{\mathrm{A}}$ and $w_{\mathrm{B}}(\varrho_{\mathrm{B}}, y) \triangleq \partial G(\varrho_{\mathrm{B}}, y)/\partial \varrho_{\mathrm{B}}$ the kinematic wave speeds of directions A and B, respectively.

First consider the case where F and G are unimodal nFDs (see Fig. 3(a)) and the buffer lane is closed. The value of the Lagrange multiplier μ^* guarantees that the optimal distribution $(\varrho^*_{\mathrm{A}}(x),\ \varrho^*_{\mathrm{B}}(y))$ satisfies (3). Given that (3) is an equality constraint, μ^* can take any value in the real line, depending on N. If μ^* is positive, then w_{A} and w_{B} must be positive for all x and y, respectively. This suggests that ϱ_{A} and ϱ_{B} should be on the left branch of F and G for all x and y, respectively; i.e., both directions of traffic should be uncongested everywhere. Contrary, if μ^* is negative, then w_{A} and w_{B} must be negative and both directions of traffic should be congested everywhere. Finally, if μ^* is zero, $|w_{\mathrm{A}}| \approx 0$ and $|w_{\mathrm{B}}| \approx 0$, i.e., both directions of traffic should be at flow capacity everywhere ($\varrho_{\mathrm{A}} = \varrho_{\mathrm{B}} \approx \varrho_{\mathrm{cr}}$) and system's throughput is maximised.

Condition (4) also implies that the most popular direction of traffic (i.e., the one with the largest number of trips f or g) should have the smallest slope (w_{A} or w_{B}, respectively) in absolute value, i.e., the densities closest to critical and flows closest to capacity. Further, it suggests that the least popular direction of traffic with the smallest number of trips should have the largest positive slope, i.e., should be on the rising branch of the FD. This result also confirms the validity of Assumption 1, implying that if $f(x)$ is large for direction A (w_{A} should be small) then $g(y)$ should be sufficient small (and w_{B} should be sufficient large). In other words, the ratio of exiting flows between A and B is equal to the reciprocal of their kinematic wave speeds.

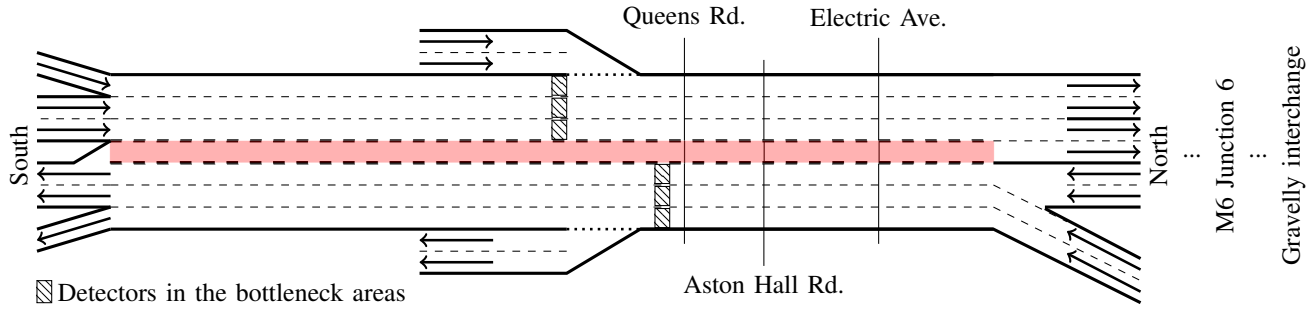

Fig. 4. Network topology of the simulated 1.1 mile tidal flow stretch of the A38(M) Aston Expressway in Birmingham, UK. The (middle) contraflow buffer zone is indicated with red colour.

(a) (b) (c)

Fig. 5. (a) Top view of A38(M) Aston Expressway at Electric Avenue; (b) gantry with SB view at around Aston Hall Rd with two lanes SB, one buffer lane, and four lanes NB; and (c) gantry with NB view at around Electric Avenue with three lanes NB, one buffer lane, and three lanes SB. ©2017 Google Earth.

Consider now the case of instability, where flow disparity is significant between the two directions of traffic, critical traffic conditions are developed in direction A while direction B free-flows as shown in Fig. 3(a) (e.g., traffic state ≪a≫ is on the congested regime while state ≪b≫ is on the uncongested regime of the nFD). In this case, the FD-based switching policy (1) opens the buffer lane for direction A and closes one lane in direction B (i.e., $u = 1$). This results in direction A operating under the eFD with number of lanes $\lambda_{\mathrm{A}} = \lambda + 1$ while B operates under the rFD with number of lanes $\lambda_{\mathrm{B}} = \lambda - 1$. This switching produces two waves as shown in Fig. 3(a), the right one (a,a') is a (accelerating) rarefaction wave and the left one (b,b') is a standing (transition) wave. The rarefaction wave forces congested state ≪a≫ in the nFD to meet state ≪a'≫ in the uncongested regime of the eFD, where flow is maintained, speed is increased while density is substantially decreased to accommodate a largest number of trips. The standing wave, with wave speed virtually zero, forces state ≪b≫ in the nFD to meet state ≪b'≫ in the uncongested regime of the rFD, where flow is maintained, speed is slightly decreased while density is slightly increased. As a special property of the triangular FD $w_{\mathrm{A}} = w_{\mathrm{B}} = w_{\mathrm{f}} > 0$ and thus the switching waves (a,a') and (b,b') imply $f(x) = g(y)$ and $\mu^* > 0$, i.e., both directions of traffic should be uncongested everywhere and should be served with the same trip rate. The case $u = -1$ can be analysed using similar arguments.

In summary, the proposed tidal flow lane control and optimality condition (4) suggest that infrastructure and densities should be managed so as to maximise flow on the direction of the motorway that contains the maximum number of desired destinations. Thus, it benefits both directions of traffic and is Pareto-optimal. Fig. 3(b) depicts the Pareto frontier of (1), i.e., the set of all Pareto efficient solutions for both directions of traffic under tidal flow lane control. Any hyperplane tangent to the Pareto frontier is a supporting hyperplane. Here supporting hyperplanes are the three cases offered in (1). Proof follows from the celebrated hyperplane separation theorem due to Minkonski [20]. Finally, it should be emphasised that maximisation of bi-directional exit flows is equivalent to the minimisation of the total time spent in the motorway network, provided control independent inflows [21].

IV. Empirical Data Analysis and Application

A. Site and Data Description

The studied site is the A38(M) Aston Expressway in Birmingham, which links the north of Birmingham City Centre to the M6 Motorway (surrounding ring-road of Birmingham). The tidal flow stretch of the A38(M) is 1.1 mile long with seven lane carriageway. The central lane acts as a contraflow buffer lane as depicted in Fig. 4. The detectors depicted in the figure are used in the simulation model. An aerial view of a short section is provided in Fig. 5(a). During AM and PM peaks the lane setup typically changes to four lanes in one direction and two lanes in the opposite direction maintaining the one lane buffer. All seven lanes are managed with lane-use control signals with green arrows and red ×s located at overhead gantries as depicted in Figs. 5(b) and 5(c).

Typically, the southbound (SB) direction is congested during the morning commute peak and the northbound (NB) during the evening peak. Real flow-speed data from six lanes (one loop detector per lane) and spanning one month, were available for the calibration of the triangular FD (Fig. 2). The six

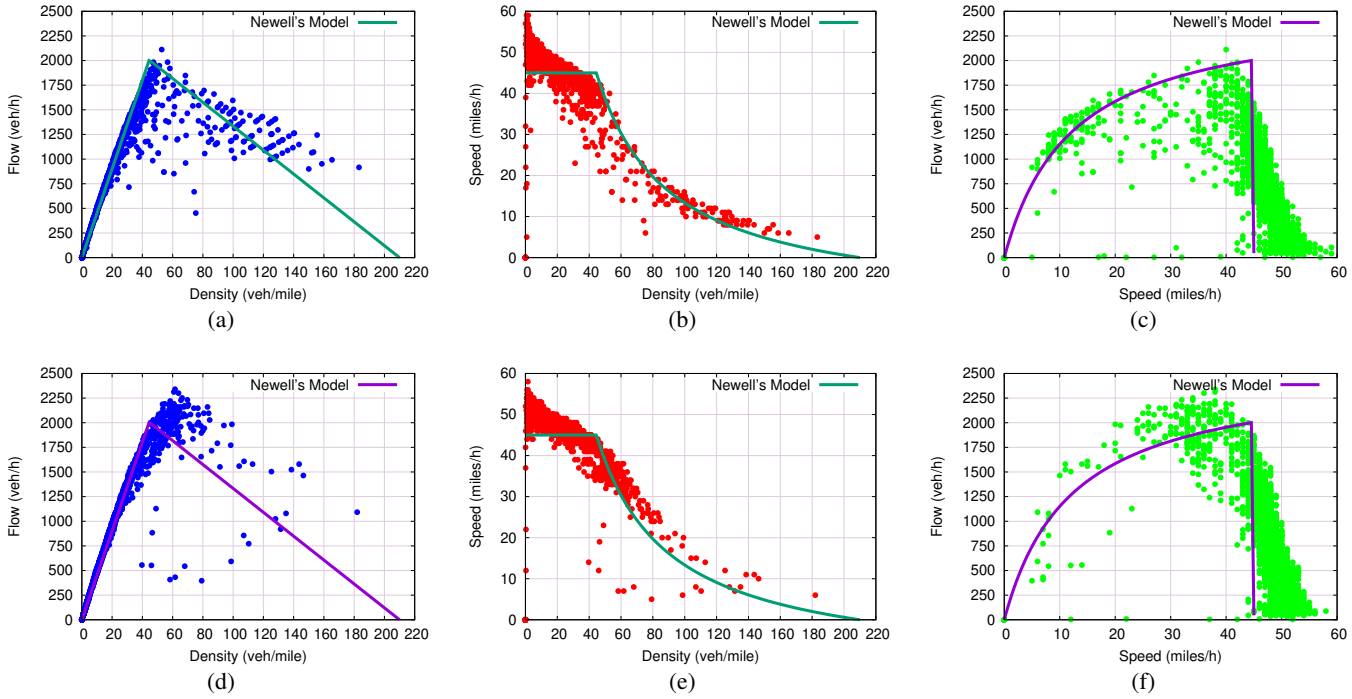

Fig. 6. Loop detector data for one lane of SB [(a)–(c)] and NB [(d)–(f)] traffic in February 2016 and approximated FDs.

detectors are located after the Gravelly interchange (Junction 6 of M6, Spaghetti Junction) towards A38(M). The empirical data were available from the Highways England "Motorway Incident Detection and Automatic Signals" (MIDAS) system in February 2016. February was selected given that it is a winter month with adverse weather and traffic conditions. The data were available in 15-min samples of flow (vehicles per 15 min) and speed (miles per 15 min). The next section analyses the empirical data collected. These data are first used in an offline mode to calibrate the FD and to obtain its critical parameters for tidal flow control and are then used as reference for adjusting some control parameters such as γ, γ^{r}, and T.

B. Empirical Data

This section shows with empirical data that A38(M) exhibits a triangular FD. We demonstrate that one fundamental diagram (set of critical parameters) can be used for both directions of traffic, although the proposed methodology can be applied with two different models, one for each direction of traffic.

Fig. 6 depicts empirical data for one month (February 2016) from one lane of both SB and NB directions of A38(M), and the corresponding FDs (flow versus density; speed versus density; and, flow versus speed). Each measurement point corresponds to 15 min samples. Fig. 6 confirms the existence of an FD for both SB and NB directions of A38(M) with moderate scatter on the congested regime. From visual inspection, it can be seen that flow capacity for both directions is observed at a critical density between 40 and 60 veh/mi, while free flow speed (the slope of the left rising branch) is around 45 mi/h. Lower flows are observed in the SB direction due to merging of A38(M) with M6 at Junction 6 (Spaghetti Junction).

Based on our analysis in Section II, we employ the piecewise linear FD (known as Newell's model), which fits well with field empirical data. The flow–density relationship reads:

$$q = \begin{cases} v_{\mathrm{f}} \cdot \varrho, & \text{if } \varrho \leq \varrho^*_{\mathrm{cr}}, \\ q_{\mathrm{cap}} \left(1 - \frac{\varrho - \varrho^*_{\mathrm{cr}}}{\varrho_{\max} - \varrho^*_{\mathrm{cr}}}\right), & \text{if } \varrho^*_{\mathrm{cr}} < \varrho \leq \varrho_{\max}, \end{cases} \tag{5}$$

with v_{f} the free-flow speed and $q_{\mathrm{cap}} = Q$ the flow capacity. Under stationary traffic conditions $q = \varrho \cdot v$, and thus the above equation implies the following speed-density relationship for the triangular FD:

$$v = \begin{cases} v_{\mathrm{f}}, & \text{if } \varrho \leq \varrho^*_{\mathrm{cr}}, \\ \frac{v_{\mathrm{f}} \cdot \varrho^*_{\mathrm{cr}}}{\varrho_{\max} - \varrho^*_{\mathrm{cr}}} \left(\frac{\varrho_{\max}}{\varrho} - 1\right), & \text{if } \varrho^*_{\mathrm{cr}} < \varrho \leq \varrho_{\max}. \end{cases} \tag{6}$$

Fig. 6 depicts these relationships for $v_{\mathrm{f}} = 45$ mi/h, $q_{\mathrm{cap}} = 2000$ veh/h/lane, $\varrho^*_{\mathrm{cr}} = 45$ veh/mi/lane, and $\varrho_{\max} = 210$ veh/mi/lane. Note that the triangle is not isoscale and that the theoretical optimal value for the critical density ϱ_{opt} is around $\varrho_{\mathrm{opt}} \approx \varrho_{\max}/5 = 42$ veh/mi/lane, approximately equal to the ϱ^*_{cr} used above.

C. Simulation Setup and Parametric Sensitivity

For testing the proposed control, the stretch of A38(M) was modelled in the microscopic traffic simulator AIMSUN [22]. We approximated the empirical data available and calibrated the observed FD in Section IV-B. Figs 7(a) and 7(b) show the flow-density diagram and Newell's model approximation (with $v_{\mathrm{f}} = 52$ mi/h, $q_{\mathrm{cr}} = 2100$ veh/h/lane, $\varrho^*_{\mathrm{cr}} = 40$ veh/mi/lane, and $\varrho_{\max} = 250$ veh/mi/lane) for the NB and SB traffic, respectively. This calibrated model approximates the Newell's model observed from the empirical data in Section IV-B (cf.

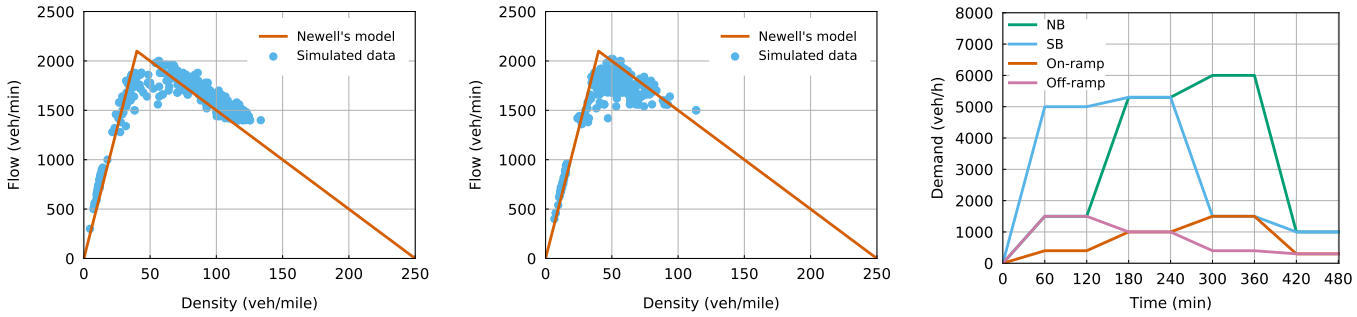

(a) (b) (c)

Fig. 7. Flow-density diagrams constructed with simulated loop-detector data and Newell's model approximation for (a) NB and (b) SB middle lanes; (c) simulated demand at the main entrances, including on/off-ramps.

Figs 7(a) and 7(b) with Figs 6(a) and 6(d)). The simulation data were obtained from loop detectors for twelve replications with different seeds. Fig. 7(c) depicts the simulated demands at both ends of the motorway for a horizon of 480 min (8 h). These trapezoidal demand profiles, including a one-hour strong demand to form congestion in both directions of traffic, were chosen so as to force the motorway going through all possible lane configurations under tidal lane control.

Note that congestion at on-ramp merges typically form at the ramp nose. However, in AIMSUN congestion forms at the merge area. To avoid fixes for the measurement at the merge area [23], the detectors were placed at the ramp gore in the NB direction. Because we work with a switching controller, the effect on the results to be presented next is a longer time for control activation and for congestion dissipation. Obviously, in practice the detectors should be placed at the ramp nose, where congestion forms, for best performance. In the SB direction, the detectors were placed upstream of the off-ramp, where weaving causes the congestion.

Based on the simulation data and diagrams of Fig. 7: $\lambda = 3$, $\varrho_{\rm cr} = \lambda \cdot \varrho^*_{\rm cr} = 120$ veh/mi (nFD with three lanes) and $\varrho^{\rm r}_{\rm cr} = (\lambda - 1) \cdot \varrho^*_{\rm cr} = 80$ veh/mi (rFD with two lanes). The control algorithm was applied for four different combinations of values of $\Delta \triangleq \gamma \varrho_{\rm cr}$ and $\Delta^{\rm r} \triangleq \gamma^{\rm r} \varrho^{\rm r}_{\rm cr}$ in order to assess its sensitivity to different switching bandwidths $\Delta_{\rm b} \triangleq \Delta - \Delta_{\rm r}$: Case I: the nominal values were used, i.e., $\gamma = \gamma^{\rm r} = 1$ and $\Delta_{\rm b} = 40$ veh/mi (nominal bandwidth); Case II) $\Delta = \frac{6}{5}\varrho_{\rm cr} = 144$ veh/mi and $\Delta^{\rm r} = \frac{4}{5}\varrho^{\rm r}_{\rm cr} = 64$ veh/mi; $\Delta_{\rm b} = 80$ veh/mi (small bandwidth); Case III) $\Delta = \frac{5}{4}\varrho_{\rm cr} = 150$ veh/mi and $\Delta^{\rm r} = \frac{3}{4}\varrho^{\rm r}_{\rm cr} = 60$ veh/mi; $\Delta_{\rm b} = 90$ veh/mi (medium bandwidth); Case IV) $\Delta = \frac{4}{3}\varrho_{\rm cr} = 160$ veh/mi and $\Delta^{\rm r} = \frac{2}{3}\varrho^{\rm r}_{\rm cr} = 53.3$ veh/mi; $\Delta_{\rm b} = 106.7$ veh/mi (large bandwidth). In addition, these three scenarios were repeated for $T \in \{10, 20, 30\}$ min. For all cases and control intervals, observations from inductive-loop detectors (shown in Fig. 4) of $\varrho_{\rm A}$ and $\varrho_{\rm B}$ were available for feedback every 1 min and aggregated to $T_{\rm m} = 15$ min.

Two other control schemes were considered namely, *optimised control* and *manual control*. The optimised control provides an upper bound of achievable performance. For manual control, the operator was allowed to switch lanes at every ten minutes through visual inspection of the motorway (to emulate empirical observations from CCTV surveillance cameras). The main drawback of manual control is that it does require operator's personal (subjective) judgement and typically has not as much freedom as in this example.

TABLE I
QUANTITATIVE MEASURES OF ASSESSMENT

Control policy	T (min)	TTS (veh×h)	Improv. (%)	STD	Average # switchings
No-control	-	2689.5	-	-	-
Manual control	10	1784.9	33.6	24.6	8
Optimised	free	1204.2	55.2	11.9	4
Case I	10	1183.3	56.0	22.1	4
(nominal	20	1186.0	55.9	22.0	4
bandwidth)	30	1343.1	50.1	104.1	4
Case II	10	1290.0	52.0	53.9	6
(small	20	1447.6	46.2	121.4	5
bandwidth)	30	1423.8	47.1	94.6	4
Case III	10	1293.8	51.9	59.3	7
(medium	20	1447.6	46.2	121.4	5
bandwidth)	30	1435.1	46.6	108.6	4
Case IV	10	1439.1	46.5	112.7	8
(large	20	1439.4	46.5	108.6	6
bandwidth)	30	1456.9	45.8	128.1	4

For all control schemes, after a decision for switching the lane configuration, a time window of one minute was provided for vehicles to exit the lane(s) to be closed for a given direction. These control schemes were compared against a *no-control* scheme in which SB and NB directions operate with three lanes and the contraflow buffer lane is closed. Note that six lanes in total were used in all control schemes, and thus the presented results are comparable.

D. Results and Sensitivity Analysis

The simulation results obtained from the average of twelve replications for each control case are shown in Table I. Clearly, the proposed strategy provides significant improvements compared to the no-control and manual control cases. As can be seen under tidal flow lane control, the Total Time Spent (TTS) is improved systematically for all scenarios (from 33% to 56%). For a given control period T, the small difference seen among Cases I–IV indicates that the strategy has low sensitivity to the chosen parameters. Moreover, although all cases show a decrease in performance for increasing T, the improvement in TTS is still substantial even for $T = 30$ min.

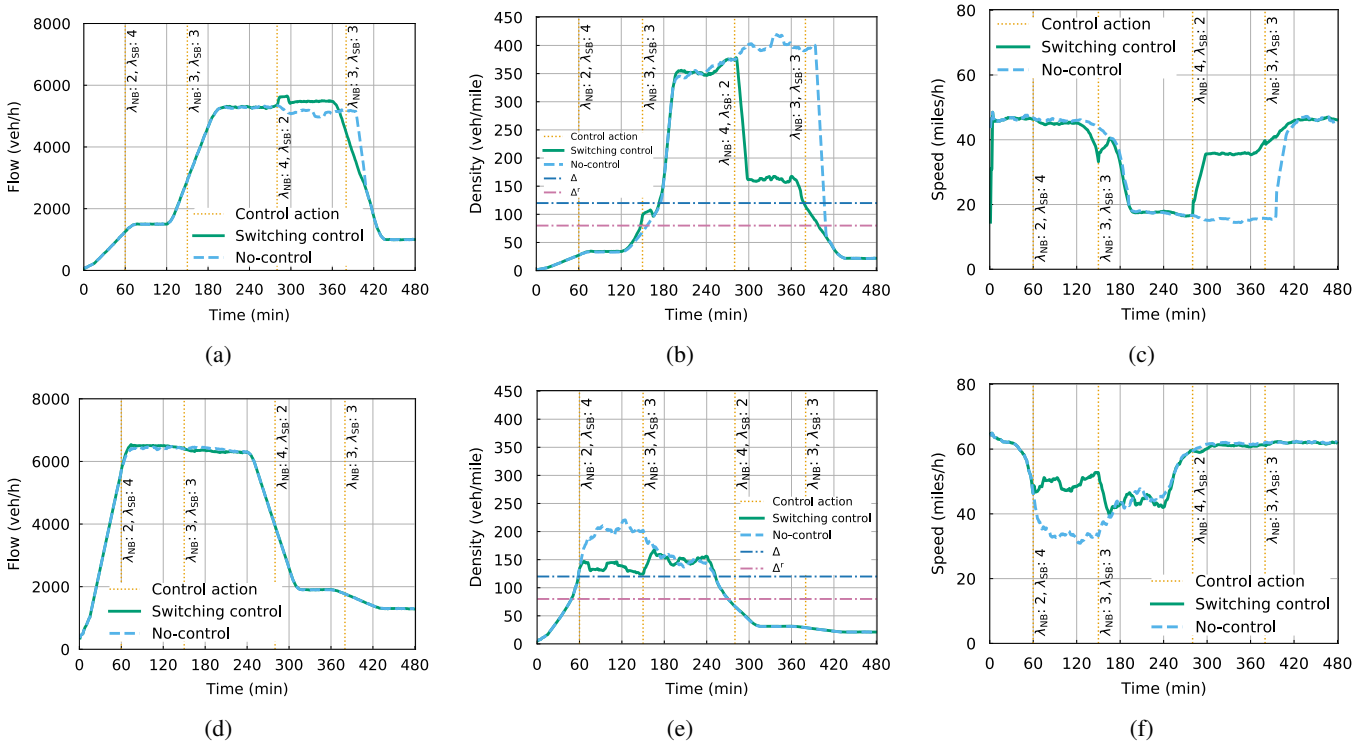

Fig. 8. Simulation results of switching control (for Case I, $T = 10$ min) and no-control: (a) flow, (b) density, and (c) speed at around the NB bottleneck location; and (d) flow, (e) density, and (f) speed at around the SB bottleneck location.

The last column in Table I reports the average (rounded up) number of control switchings over twelve replications. As can be seen, the average number of switchings is between four and six for most cases and different T. The combination of small T with larger bandwidths in Cases III and IV indicates seven to eight switchings, which is acceptable.

The optimised control case with free T excels and, although these benefits are hardly attainable in reality, they were achieved closely by the proposed switching policy in most scenarios, particularly for Case I. Manual control under performs expressively compared to the other control cases. The attempt to improve performance under manual control when both directions of traffic were congested lead to an unstable behaviour that resulted in an increased number of switches. The still satisfactory performance of manual control is due to operator who was well trained and had good knowledge of the simulated scenario. Indeed, to excel, operators of tidal facilities need many years of experience and training to achieve good performance. The demonstrated improvements underline the superiority of appropriate real-time tidal flow lane control and efficient use of the available infrastructure, which is underutilised in the no-control case.

To further demonstrate the performance of the proposed switching policy, Figs 8(a)–(f) show, respectively, the NB and SB flow, density, and speed at around the bottleneck locations (see Fig. 4) for Case I with $T = 10$ min alongside the no-control case. The control action vertical lines indicate the switching time and are labeled with the number of lanes for the control scenario in NB and SB directions after switching. The data corresponds to a replication with its results closest to the average values in Table I.

The improved TTS stems from the increased throughput in the controlled scenario enabled by the proposed strategy with only four switches. The improvement is reflected by higher flows between around 290 to 380 mins in the NB direction (Fig. 8(a)) and between around 60 to 120 mins in the SB direction (Fig. 8(d)). Right at the beginning of the simulation, the high demand in the SB direction (Fig. 7(c)) causes a rapid increase in density (Fig. 8(e)). As a consequence, the control strategy closes one lane in the NB direction and opens the buffer lane to the SB direction. The peak period in the SB direction is extended by a simultaneous high demand in the NB direction that results in congestion at both directions. In this case, there is no much that the control strategy can do and the *do nothing* policy is applied, i.e., both directions are allocated with three lanes each. The control strategy is able to reduce density, while in the no control scenario density remains at high values for the whole peak period. Next, the reduction in demand in the SB direction and high demand in the opposite direction call for an extra lane in the NB direction. A increase of flow and reduction of density in the NB is immediately observed after the switch, despite the high demands involved. In both directions, the average speed is higher with control most of the time, but clearly during the peak-periods (Figs 8(c) and 8(f)).

Fig. 9 shows the flow, density and speed of the SB direction of two other control strategies: optimised and manual control. The lines of Δ and Δ^{r} in Figs 9(b) and 9(e) are shown for reference only. It is clear from Figs 9(a)–9(c) that the optimised control favour the NB direction compared to Figs 8(d)–

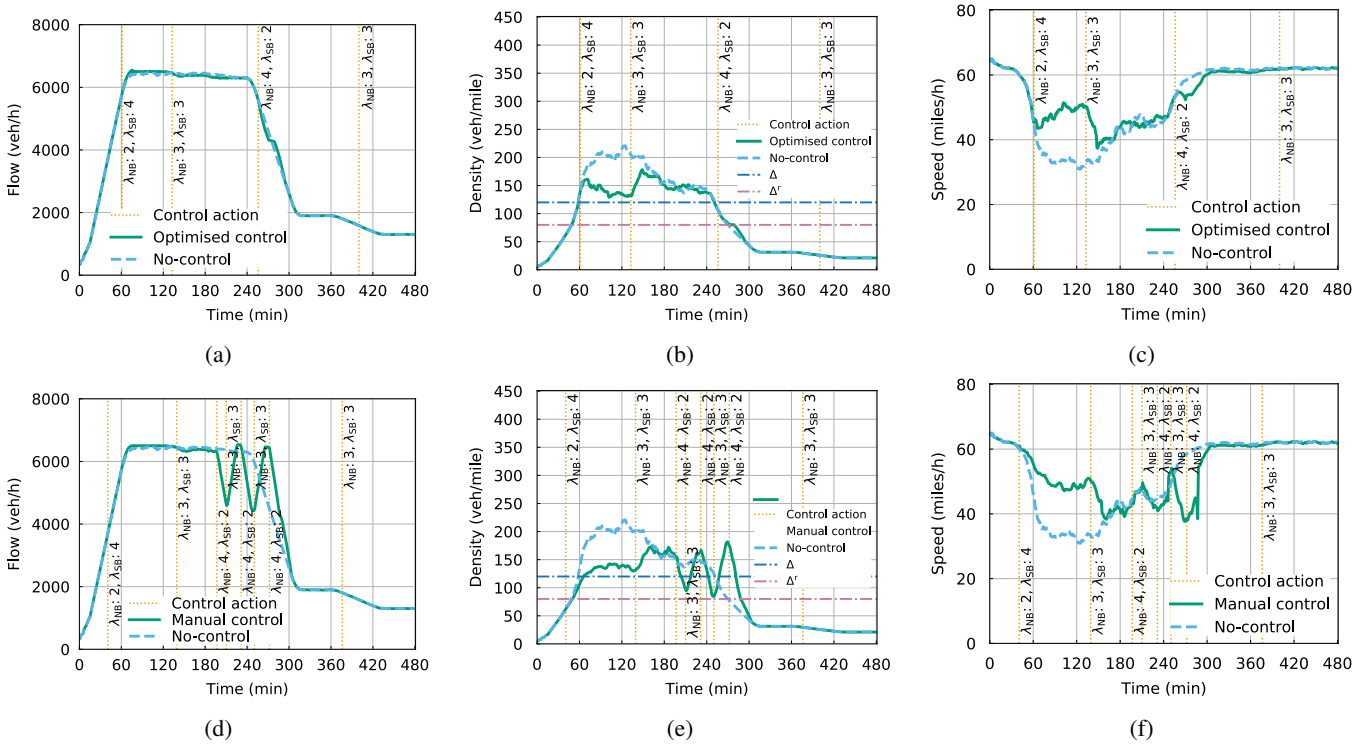

Fig. 9. Simulation results for the Southbound (SB) direction only, with optimised, manual, and no-control. Optimised control: (a) flow, (b) density, and (c) speed at around the bottleneck location. Manual control: (d) flow, (e) density, and (f) speed at around the bottleneck location.

8(f) despite the similar TTSs obtained. For manual control, the intervention of the operator causes a visible degradation of traffic conditions at around 200 to 280 min, noticeable specially in Fig. 9(f) that shows an increased duration of low speeds. Similar conditions are also observed in the NB direction. Remarkably the proposed switching strategy deliver substantial improvements in performance, despite the presence of exogenous flows at the on/off-ramps.

An aggregated measurement period of $T_{\rm m} = 5$ mins was also used for all scenarios (Cases I–IV for all T) without major differences in performance. Bandwidths shifted down and up with respect to the critical density were tried and did not result in major differences as well. These additional simulations also demonstrated the robustness to control parameter variations for the simulated scenarios. The lines of Δ and $\Delta^{\rm r}$ in Figs 8(b) and 8(e) suggest that there may is still be room for tuning their values and obtain slightly better TTS values, e.g., via an adaptive fine-tuning algorithm [24].

V. Conclusions and Discussion

This paper presented a practicable FD-based switching policy for smooth and efficient motorway tidal flow operations. The proposed state-feedback policy relies on real-time observations of density only and certain properties of the fundamental diagram of traffic. It does not rely on any forecasts nor real-time optimisation, and thus it is applicable in real-time to improve efficiency of motorway networks. It is also expected to reduce the cost to manage and operate tidal flow facilities. A microsimulation study of a site currently managing tidal flows, the A38(M) in Birmingham, UK, was used to demonstrate the operation of the proposed policy. Real empirical data were used to calibrate the required fundamental diagrams. The simulation results confirmed an increase of motorway throughput and a smooth operation of the strategy. Parametric sensitivity analysis was employed to demonstrate the robustness properties of the switching policy to parameter variations.

This work also offered some theoretical results on how the infrastructure should be managed to accommodate the distribution of densities that maximises the bi-directional total outflow. The pursued theoretical analysis, which is based on the Kinematic Wave theory, has shown that the proposed policy leads (under certain conditions) to bi-directional motorway throughout maximisation and total time spent minimisation. The problem of bi-directional throughput maximisation was formulated as a constrained optimisation problem and first-order necessary conditions were derived. The obtained optimality conditions imply that the direction of traffic with the largest number of trips should have the smallest slope (kinematic wave speed) in absolute value, i.e., the densities closest to critical and flows closest to capacity. Further, it suggests that the direction of traffic with the smallest number of trips should have the largest positive slope, i.e., should be on the rising branch of the FD. An alternative interpretation of the optimality conditions suggests that the ratio of exiting flows between the two directions of traffic is equal to the reciprocal of their kinematic wave speeds.

In summary, the obtained optimality conditions suggest that infrastructure and densities should be managed so as to maximise flow on the direction of motorway that contains the maximum number of desired destinations. Remarkably, the proposed switching policy provides Pareto efficient solutions

for both directions of traffic under tidal flow lane control. Well-designed tidal flow management policies would ideally conform to these conditions in order to be Pareto-optimal and benefit both directions of traffic.

We envision emerging vehicle-infrastructure integration systems, which support vehicle-to-vehicle and vehicle-to-infrastructure communications, amalgamated with reversible lanes appropriately controlled to ensure safe operation of tidal flows and mitigate congestion.

REFERENCES

[1] M. Papageorgiou, C. Diakaki, V. Dinopoulou, A. Kotsialos, and Y. Wang, "Review of road traffic control strategies," *Proc. IEEE*, vol. 91, no. 12, pp. 2043–2067, 2003.

[2] R. C. Carlson, I. Papamichail, M. Papageorgiou, and A. Messmer, "Optimal mainstream traffic flow control of large-scale motorway networks," *Transportation Research Part C*, vol. 18, no. 2, pp. 193–212, 2010.

[3] J. Obenberger, "Managed lanes," *Public Roads*, vol. 68, no. 3, pp. 48–55, 2004.

[4] B. Wolshon and L. Lambert, "Reversible lane systems: synthesis of practice," *Journal of Transportation Engineering*, vol. 132, no. 12, pp. 933–944, 2006.

[5] L. Lambert and B. Wolshon, "Characterization and comparison of traffic flow on reversible roadways," *Journal of Advanced Transportation*, vol. 44, no. 2, pp. 113–122, 2010.

[6] J. J. Wu, H. J. Sun, Z. Y. Gao, and H. Z. Zhang, "Reversible lane-based traffic network optimization with an advanced traveler information system," *Engineering Optimization*, vol. 41, no. 1, pp. 87–97, 2009.

[7] M. Hausknecht, T. Au, P. Stone, D. Fajardo, and T. Waller, "Dynamic lane reversal in traffic management," in *14th International IEEE Conference on Intelligent Transportation Systems*, 2011, pp. 1929–1934.

[8] H. L. Khoo and Q. Meng, "Characterization and comparison of traffic flow on reversible roadways," *The IES Journal Part A: Civil & Structural Engineering*, vol. 1, no. 4, pp. 291–300, 2008.

[9] Q. Meng and H. L. Khoo, "Optimizing contraflow scheduling problem: model and algorithm," *Journal of Intelligent Transportation Systems*, vol. 12, no. 3, pp. 126–138, 2008.

[10] T. S. Glickman, "Heuristic decision policies for the control of reversible traffic links," *Transportation Science*, vol. 7, no. 4, pp. 362–376, 1973.

[11] J. Zhao, W. Ma, Y. Liu, and X. Yang, "Integrated design and operation of urban arterials with reversible lanes," *Transportmetrica B*, vol. 2, no. 2, pp. 130–150, 2014.

[12] W. W. Zhou, P. Livolsi, E. Miska, H. Zhang, J. Wu, and D. Yang, "An intelligent traffic responsive contraflow lane control system," in *IEE Vehicle Navigation & Information Systems Conference*, 1993, pp. 174–181.

[13] D. Xue and Z. Dong, "An intelligent contraflow control method for real-time optimal traffic scheduling using artificial neural network, fuzzy pattern recognition, and optimization," *IEEE Transactions on Control Systems Technology*, vol. 8, no. 1, pp. 183–191, 2000.

[14] J. R. D. Frejo, I. Papamichail, M. Papageorgiou, and E. F. Camacho, "Macroscopic modeling and control of reversible lanes on freeways," *IEEE Trans. Intell. Transp. Syst.*, vol. 17, no. 4, pp. 948–959, 2016.

[15] K. Ampountolas, H. S. Furtado, and R. C. Carlson, "Motorway tidal flow lane control," *IFAC-PapersOnLine*, vol. 51, no. 9, pp. 279–284, 2018.

[16] G. F. Newell, "A simplified theory of kinematic waves in highway traffic Part I: General theory," *Transportation Research Part B*, vol. 27, pp. 281–287, 1993.

[17] M. J. Lighthill and G. B. Whitham, "On kinematic waves II. A theory of traffic flow on long crowded roads," *Proceedings of the Royal Society of London A*, vol. 229, no. 1178, pp. 317–345, 1955.

[18] P. I. Richards, "Shock waves on the highway," *Operations Research*, vol. 4, no. 1, pp. 42–51, 1956.

[19] J. Banks, "Review of empirical research on congested freeway flow," *Transportation Research Record*, vol. 1802, pp. 225–232, 2002.

[20] H. G. Eggleston, *Convexity*, ser. Cambridge Tracts in Mathematics. Cambridge University Press, 1958.

[21] M. Papageorgiou and A. Kotsialos, "Freeway ramp metering: An overview," *IEEE Trans. Intell. Transp. Syst.*, vol. 3, no. 4, pp. 271–281, 2002.

[22] Transport Simulation Systems, *AIMSUN Users' Manual v. 8*, Barcelona, Spain, 2015.

[23] E. R. Müller, R. C. Carlson, W. Kraus, and M. Papageorgiou, "Microsimulation analysis of practical aspects of traffic control with variable speed limits," *IEEE Trans. Intell. Transp. Syst.*, vol. 16, no. 1, pp. 512–523, 2015.

[24] A. Kouvelas, K. Aboudolas, E. B. Kosmatopoulos, and M. Papageorgiou, "Adaptive performance optimization for large-scale traffic control systems," *IEEE Trans. Intell. Transp. Syst.*, vol. 12, no. 4, pp. 1434–1445, 2011.

Konstantinos Ampountolas (S'04-M'09) received the Dipl.-Ing. degree in production engineering and management (1999), the M.Sc. degree in operations research (2002), and the Ph.D. degree in engineering (2009), all from the Technical University of Crete, Greece. He is currently a Senior Lecturer with the James Watt School of Engineering at the University of Glasgow, United Kingdom. He was a research fellow at École Polytechnique Fédérale de Lausanne (2012-2013), Switzerland, visiting researcher scholar at the University of California, Berkeley, CA (2011), and post-doctoral researcher at the Centre for Research and Technology Hellas, Greece (2010). He was also short-term visiting professor at Technion–Israel Institute of Technology, Israel (2014), and the Federal University of Santa Catarina, Florianópolis, Brazil (2016; 2019). His research interests include automatic control and optimisation with applications to traffic networks and transport systems. Dr Ampountolas serves as an associate editor of the *Journal of Big Data Analytics in Transportation* and on the editorial advisory boards of *Transportation Research Part C*, *Transportation Research Procedia*, and *Data in Brief*.

Joana Alves dos Santos is an undergraduate student of Control and Automation Engineering in the Department of Automation and Systems at the Federal University of Santa Catarina, Florianópolis, Brazil. Since 2017 she works as a research assistant at the Department of Automation and Systems funded by the The National Council for Scientific and Technological Development (CNPq). Her research interests include control and formal verification of traffic systems involving automated vehicles.

Rodrigo Castelan Carlson (M'12) received the Bel.Eng. degree in control and automation engineering and the Me.Eng. degree in electrical engineering from the Federal University of Santa Catarina, Brazil, in 2004 and 2006, respectively; the B.B.A. degree in Business Administration from the Santa Catarina State University, Brazil, in 2006; and the Ph.D. degree from the Technical University of Crete, Greece, in 2011. From 2012 to 2015 he was an Assistant Professor with the Mobility Engineering Center, and since 2015 he has been an Assistant Professor with the Department of Automation and Systems at the Federal University of Santa Catarina. His research interests include control and optimization applications to traffic systems. In these areas, he has been serving as a reviewer for journals and conferences as well as a consultant. He also served as the member of program committees for several conferences, guest editor for journals, and since 2018 he is serving as associate editor for the *IET Intelligent Transport Systems* journal.

Dr. Carlson received a scholarship for postgraduate studies abroad from The Capes Foundation, Ministry of Education of Brazil (2007–2011) and the Gold Medal of the Young European Arena of Research 2010 in the pillar "Mobility and Intermodality". In 2017 and in 2018 he was awarded the prize ANPET of Scientific Production. Since 2015 he holds the status of researcher from The National Council for Scientific and Technological Development (CNPq).